In situ snow water equivalent observations in the US Arctic

Svetlana Stuefer, Douglas L. Kane and Glen E. Liston

ABSTRACT

This paper summarizes 12 years of snow water equivalent (SWE) observations collected in the data-sparse region of Arctic Alaska, United States. The *in situ* observations are distributed across a 200 × 300 km domain that includes the Kuparuk River watershed from the Brooks Range to the Beaufort Sea coast. Data collection methods and analyses were classified to distinguish between snow observation sites representing regional- and local-scale variability. Average SWE for the entire domain ranges from 92 mm in 2008 to 148 mm in 2011. Regional end-of-winter SWE indicates that both the extreme high SWE in 2009 and 2011 and the extreme low SWE in 2008 occurred during recent and alternating years, suggesting the limitations of 12 years of data for detecting SWE trends. By assimilating the observational datasets into SnowModel, hourly 100 m gridded SWE distributions for the central Alaska Arctic were created to provide a best-fit to the observations where and when they occur. The model simulations highlight how observed SWE data can be used as a surrogate for the more problematic winter precipitation measurements. The resulting SWE distributions are readily available to support ecological and hydrologic studies in this region.

Key words | Arctic, climate, North Slope of Alaska, snow depth, snow water equivalent

Svetlana Stuefer (corresponding author)
Douglas L. Kane
Department of Civil and Environmental Engineering,
Water and Environmental Research Center,
University of Alaska Fairbanks,
Fairbanks,
Alaska,
USA
E-mail: *sveta.stuefer@alaska.edu*

Glen E. Liston
Cooperative Institute for Research in the Atmosphere,
Colorado State University,
Fort Collins,
CO,
USA

INTRODUCTION

Climate over the Arctic has experienced significant changes during the past few decades. These changes include considerable winter and spring warming (Serreze *et al.* 2000; Chapin *et al.* 2005; Hinzman *et al.* 2005), winter and fall precipitation increase (Christensen *et al.* 2007; Räisänen 2008; Deser *et al.* 2009), reduction in snow-cover extent and increase in snow depth (Räisänen 2008; Brown & Robinson 2011; Liston & Hiemstra 2011), sea-ice cover extent decrease (Stroeve *et al.* 2008; Deser *et al.* 2009), polar ice sheet and glacier melting and ground temperature rising and permafrost thawing (Hinzman *et al.* 2005; IPCC 2007; Romanovsky *et al.* 2007). Temperature increases and associated climate feedbacks (Chapin *et al.* 2005; Euskirchen *et al.* 2007) are expected to continue. This warming trend will impact the structure, function and stability of both terrestrial and aquatic ecosystems and alter land–ocean interaction throughout the Arctic (ACIA 2005; White *et al.* 2007; McGuire *et al.* 2009).

Observations provide evidence and foundation for scientific investigations. Most of the uncertainties in our understanding of the Arctic climate system arise from a sparse observational network and the short period of observations in remote northern regions. A number of efforts have been undertaken to address these challenges, including research field campaigns to collect new data and programs to maintain existing observational networks (Shiklomanov *et al.* 2002; Hinzman *et al.* 2005; Romanovsky *et al.* 2007). This paper presents one of these efforts, a long-term snow dataset collected during the last decade in Arctic Alaska, USA.

Assessment of snow accumulation and snowmelt is critical information in Arctic and alpine hydrologic studies. The seasonal snowpack constitutes winter storage of precipitation, induces considerable differences in surface energy balance and affects the amount of soil desiccation that occurs within the organic layer overlying the permafrost

doi: 10.2166/nh.2012.177

(Kane *et al.* 1978). Ecologically, snowmelt guarantees that water will be available to plants at the beginning of the short Arctic summer. Snowmelt is often the major hydrological event each year. For many larger river watersheds, such as the Yenisey, Lena and Ob Rivers in Siberia or the Colville and Kuparuk Rivers in Alaska, the peak discharge of record is due to snowmelt. In addition, difficulties in quantifying snow precipitation and sublimation make ground snow measurements the most reliable observational component of the net winter water budget.

Observations of snowpack in the US Arctic began in the mid-1900s, reported by Benson (1982), Benson & Sturm (1993), Sturm & Benson (2004), Olsson *et al.* (2002) and others. Kane *et al.* (1991) initiated a long-term observation data collection for the research community in 1985, an effort supported by federal and state funding agencies for over two decades. This data collection included hydrological and meteorological observations spatially distributed across the central Alaska Arctic.

We present a classification for snow data collected from 1996 to 2011 in the Alaska Arctic by faculty, staff and students of the Water and Environmental Research Center, University of Alaska Fairbanks. We describe snow water equivalent (SWE) conditions observed in the area over the last decade, and discuss extreme high and low snow years. In addition, we provide an example of observed data assimilation into a physically based, spatially distributed snow model. This information can be useful for model validation/calibration, can improve algorithms for remote sensing data interpretations and can contribute to the understanding of snow, weather and terrain interactions in the windy (generally treeless) Arctic environment.

DATA LOCATION

The snow survey data were collected in the central part of the Alaska Arctic. Figure 1 presents the spatial distribution of 166 snow survey sites, covering an extensive region that transitions from the continental divide of the Brooks Range to the coast of the Arctic Ocean.

The snow survey sites were chosen to represent snow characteristics over a wide range of vegetation and terrain conditions at elevations ranging from 5 to 1,478 m (Figure 1). The entire region is underlain with continuous permafrost that reaches a maximum thickness of 600 m near Prudhoe Bay on the coast. The area is treeless, except for a few isolated riparian areas in the foothills. Shrubs (0.4–1.0 m tall) are common throughout the watersheds, with higher densities in the foothills. The active layer is typically about 50 cm (but varies considerably due to vegetation, soil moisture, soil type, aspect, slope, etc.), with extensive surficial organic soils overlying mineral soils (Slaughter & Kane 1979). Lakes can be found throughout the region, but they exist in much greater numbers on the coastal plain. Streams are predominantly north draining and some have extensive aufeis (Slaughter & Benson 1986). Air temperature is typically below freezing by mid-September (Olsson *et al.* 2002), and breakup occurs from early May to early June. It can snow on any day of the year; three or four snow events usually occur during summer.

One of the rationales for the site location selection was to provide adequate input to hydrologic models. A large part of the study area, located in the foothills and mountains of the Brooks Range, has a myriad of rolling hills with relatively shallow snow on the ridges and deeper snow in the valley bottoms and leeward slopes. The resultant heterogeneous spatial distribution of SWE exerts important controls on the snow-cover depletion during snowmelt, causing a more gradual regional albedo decline during melt while at the same time accelerating snowmelt over the remaining local snow cover than if the snow were more evenly distributed (Shook *et al.* 1993; Liston 1995, 1999, 2004). Observations show that areas with deeper snow melt completely several days or weeks later than areas with shallower snow (Hinzman *et al.* 1990; Marsh & Pomeroy 1995), affecting the timing of peak snowmelt in small streams. Some of the snow sites were placed to capture the local snow conditions of ridges and valley bottoms. Other sites were placed so that they would be representative of the larger areas and to capture regional spatial trends.

DATA COLLECTION METHODS

Snow surveys were made at designated locations throughout the domain to determine snow depth, as well as vertically

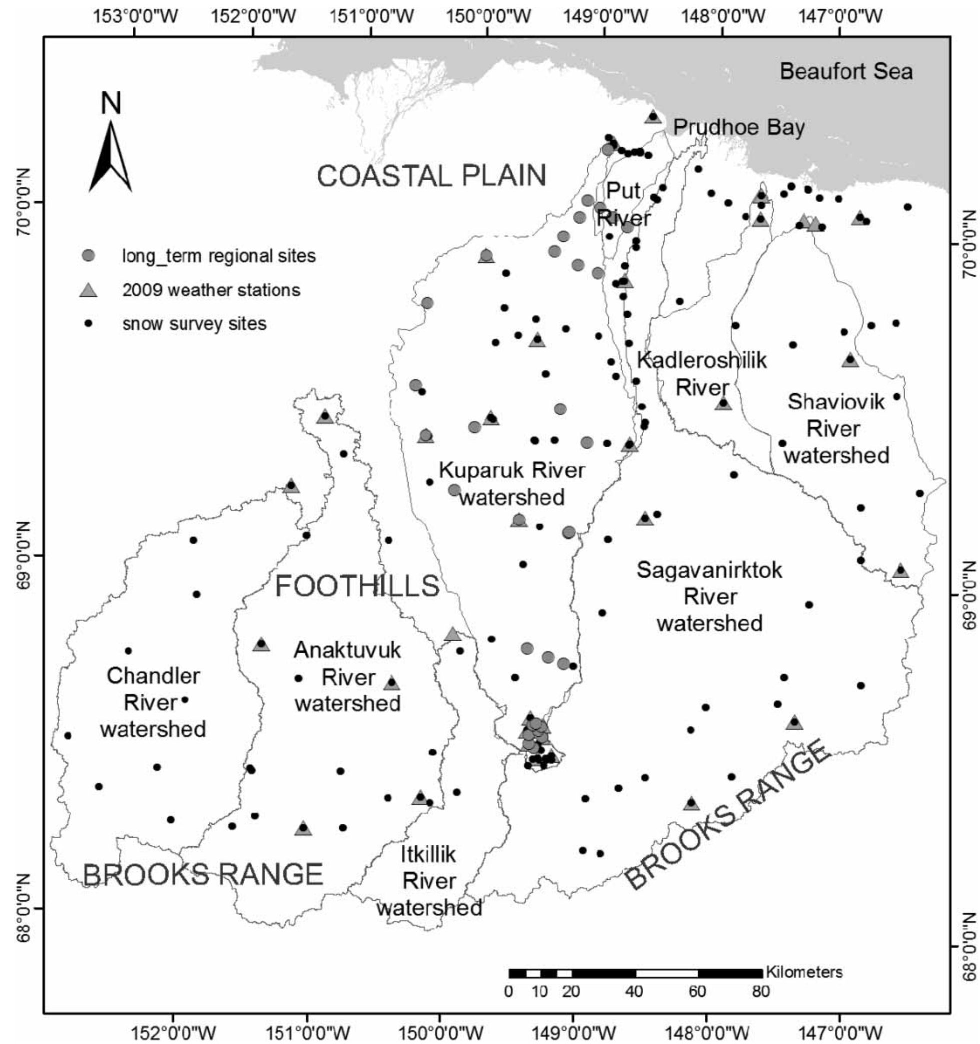

Figure 1 | Location of the all-snow survey sites (dots) and weather stations (triangles) in central Alaska Arctic. Weather stations are shown as of spring 2009. Long-term regional snow survey sites are highlighted by the grey large circle.

integrated density and SWE. Except when making ablation measurements, most of the sites were visited once a year near the peak of snow accumulation (generally the last week of April). Our observations show that the onset of ablation in this domain is typically in May. The end of April is a good time to capture end-of-winter SWE. March, April and May are often the months of lowest precipitation, and therefore there is usually little accumulation between the end-of-winter snow surveys and the onset of ablation. There are always exceptions, however; in 2007 the end of April SWE observations at the coastal plain should be corrected for the heavy snowfalls in early May of that year.

Our snow surveys include snow density and snow depth measurements collected over a 50 m distance; this technique is often referred to as 'double sampling'. The Alaska snowpack is extremely heterogeneous, with snow depth being more variable than density (Benson & Sturm 1993; Sturm *et al.* 2010). Rovansek *et al.* (1993) showed that double sampling provides improved SWE estimates; they recommended sampling 12–15 snow depths for each snow core. This optimal ratio of snow depths to water equivalent, however, appeared to vary greatly (from 1 to 23), depending on site, weather and snow conditions. We currently use an optimal ratio of 10, that is, 50 depths accompany five snow cores.

Snow cores are sampled using a fiberglass tube (Adirondack) with an inside area of 35.7 cm^2, equipped with metal teeth on the lower end to cut through dense layers of snow. The advantage of the Adirondack for shallow snowpack is that its diameter is larger than many other types of snow tubes (such as the Mt Rose); it therefore provides a larger sample of the shallow Arctic snowpack. Five snow cores are usually taken to estimate average snow density. We use constant 50 m lengths for the snow depth course, with a 1 m sampling interval along an L-shaped transect. Twenty-five depth measurements are made on each leg of the L; this strategy is used to account for the presence of snowdrifts in the area of measurement.

SWE is defined as:

$$\mathrm{SWE} = \frac{h\rho_\mathrm{s}}{\rho_\mathrm{w}} \tag{1}$$

where ρ_s is average snow density from the five snow core samples, ρ_w is water density and h is an average of 50 snow depths.

ACCURACY OF OBSERVATIONS

Today, both SWE and snow depth measurements are used as calibration and validation data against which other ground-based techniques (e.g. snow pillows, ground-based LIDAR, precipitation gauges) or airborne and satellite sensors are evaluated. The accuracy of SWE and snow density measurements obtained with a snow sampler has been widely discussed in the past (e.g. Work *et al.* 1965; Woo 1997). Woo (1997) showed that a larger tube diameter increases the accuracy of density determination; Woo also showed that the Canadian sampler (similar to the Adirondack in diameter) captures snow density within 5% of snow pit estimates. Our field comparison of Adirondack-to-snow-pit density gives similar results.

The accuracy of a single snow depth measurement depends on (a) the nature of the snowpack and the material underneath it; (b) the instrument used to make the measurement; and (c) the human factor. In areas containing well-developed organic material on top of mineral soils (Figure 2(a)), snow depth can be overestimated (Berezovskaya & Kane 2007). The density of the organic layer tends to be similar to the density of the depth hoar layer at the bottom of the snowpack. While measuring, the probe can easily penetrate low-density organic material so this additional depth from 2 to 20 cm is inadvertently incorporated into the snow depth measurement. Layers of ice within or on the bottom of the snowpack produce an error with opposite sign, as shown in Figure 2(b). Any type of correction to existing snow depth records is difficult to perform, because the error varies strongly from observer to observer and depends on snow and soil conditions at each site. Studying the effect of snow depth error on SWE of tundra snow, Berezovskaya & Kane (2007) concluded that the SWE estimated with the double-sampling technique has an accuracy of $\pm$10%.

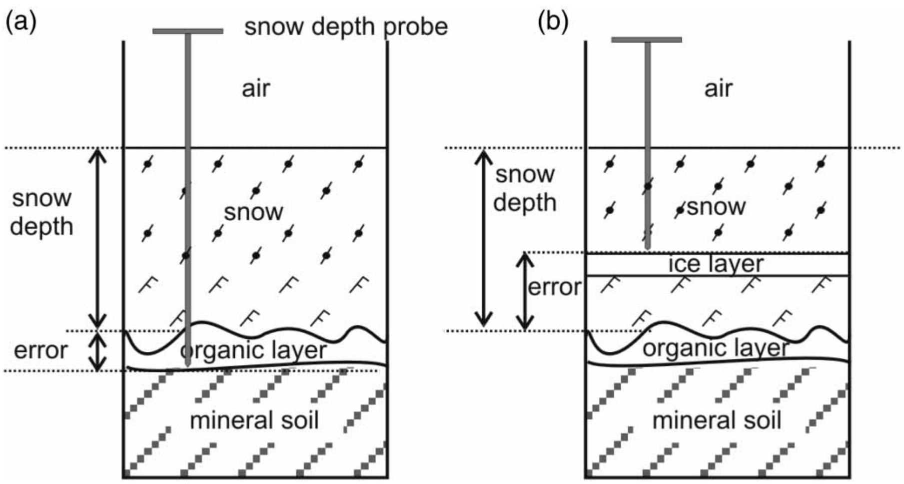

Figure 2 | Schematic diagram of the snow depth measurements and possible errors associated with over- and underestimate of snow depth.

Interpretation of the field snow data is tied to the scaling concept of 'spacing, extent and support' (Skoien & Bloschl 2006). Spacing is the average distance between snow measurements (1 m), extent is the size of the domain sampled (50 m in the L-shaped pattern) and support is the averaging area of one measurement (area of the snow depth probe or density corer).

The question of interest for this paper is how representative is the mean snow depth from our sampling extent compared to the mean snow depth over the surrounding area. The starburst pattern was developed to extend the sampling extent over a circle 100 m in diameter (Figure 3). Snow depths along four beams (N/S, E/W, NE/SW and SE/NW), each 100 m long, were measured at 1 m spacing, resulting in 404 measurements at each site. We conducted this experiment in 2005 and 2007 at three different locations. The subsets of 50 measurements that represent the L-shaped sampling at the snow survey site were extracted from the starburst pattern. A comparison of mean snow depth from the 50 measurements to the entire starburst at several locations is shown in Table 1. In most of the cases, mean snow depth from the 50 measurements is within 5% of the population mean. There are two values that are on the low end (89 and 93%) and one value that is on the high end (106%). The general interpretation is that the 50 measurements of the L-shaped scheme give a reasonable estimate of the mean snow depth within a 100-m-diameter circle.

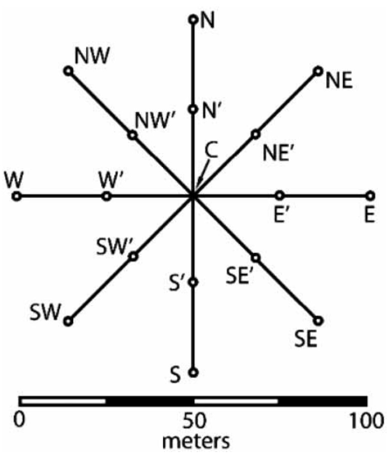

Figure 3 | Starburst sampling diagram for snow depth measurements ($n = 404$) at an intensive site. Mean snow depth of the L-shaped sampling configurations ($n = 50$) is compared with mean snow depth of all points.

Table 1 | A comparison of mean and standard deviation of L-shaped transects ($n = 50$) to the entire starburst dataset ($n = 404$). Sampling diagram and corresponding abbreviations are defined on Figure 3

Subset	No. of Points	Mean (cm)	Mean (%)	Std. Dev. (cm)
Entire Starburst at West Slope	404	49.8	100	8.1
L-Shaped Pattern, 25 m × 25 m				
N' to C to E'	50	50.3	101	10.4
E' to C to S'	50	47.5	95	8.1
S' to C to W'	50	44.1	89	6.3
W' to C to N'	50	47.2	95	8
NE' to C to SE'	50	49.4	99	7.2
NW' to C to SW'	50	49.2	99	7.1
NE' to C to NW'	50	51.0	102	7.1
SW' to C to SE'	50	47.2	95	7.1
Entire Starburst at Valley Bottom	404	43.6	100	9.2
L-Shaped Pattern, 25 m by 25 m				
N' to C to E'	50	43.7	100	7.0
E' to C to S'	50	42.3	97	6.7
S' to C to W'	50	44.6	102	8.0
W' to C to N'	50	46.1	106	7.9
NE' to C to SE'	50	42.1	97	6.5
NW' to C to SW'	50	41.4	95	7.1
NE' to C to NW'	50	42.7	98	5.7
SW' to C to SE'	50	40.8	93	7.7

RESULTS

The total number of snow survey sites increased significantly from six sites in 1996 to more than 100 in 2006–2010 (Figure 4; Table 2). Originally, most of the sites were located in the Kuparuk River and Putuligayuk (Put) River watersheds (Figure 1). In 2006, data collection extended to the east to the watersheds of the Sagavanirktok, Kadleroshilik and Shaviovik Rivers. In 2009, new sites were established in the watersheds of the Anaktuvuk, Itkillik and Chandler Rivers. Most of the sites are accessible only by helicopter or snow machine. Some of the remote sites were not visited every year because of the harsh weather conditions and other logistical considerations.

These snow survey data can be investigated to quantify snow-cover variability at different spatial scales (McKay & Gray 1981) including: the micro-scale, where characteristic

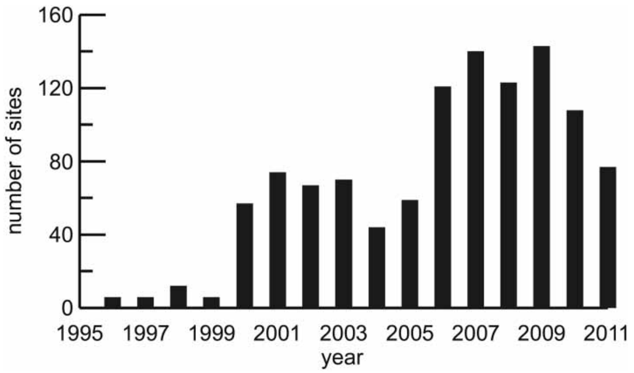

Figure 4 | Number of snow survey sites visited each year from 1996 to 2011. The earlier years of 1996–1999 lacked a sufficient number of stations for regional analysis.

Table 2 | Summary of regional SWE (mm)

Year	Total number of sites	Number of stations regional, long-term	Sample mean (mm)	Sample mean (% of mean)	Standard deviation (mm)
1996	6	3			
1997	6	2			
1998	12	4			
1999	6	1			
2000	57	25	115	102	39
2001	74	31	109	96	28
2002	67	28	109	96	35
2003	70	30	120	106	32
2004	44	15	104	92	26
2005	59	31	108	96	32
2006	121	30	100	88	26
2007	140	31	104	92	32
2008	123	29	92	81	27
2009	143	30	141	124	27
2010	108	12	105	93	34
2011	77	11	148	131	47
Mean			113		32

linear distances of 1–100 m are represented by variability from single SWE measurements; the meso-scale, where characteristic linear distances of 100–1,000 m are not captured by our measurements; and the macro-scale, where characteristic linear distances of 10–100 km are represented by variability from all the sites.

Snow-cover variability and the corresponding length scales depend on many factors, including the variability caused by micro-topography (rocks, tussocks or channels); metamorphism and ablation; snow redistribution by wind; and the nature and frequency of storms and orographic effects. Being the end-product of all these factors, snow variability at some sites is more representative of the micro-topography. At other sites, snow variability captures snowdrifts or scour zones that have resulted from complex snow–topography–wind–vegetation interactions. There are also sites that can be used to represent the areal snow variability of a larger region. Our general intent is to focus on this last class to obtain the most-representative areal SWE, assess the temporal variability of SWE during the last decade and compare the SWE with other climatic records. Since repeated *in situ* observations of such a large domain are rarely available in the Arctic, we believe that this information can be useful to both the scientific and engineering communities.

Classification of snow survey sites

Prior to analysis, snow survey sites were generalized into two classes to represent local and regional snow conditions. A local site is defined to represent snow variability associated with snow accumulation in the topographic depressions, scour zones on the ridges and deeper snow in gullies or the valley bottoms. The regional sites are chosen to represent snow conditions over the larger area, with characteristic linear distances of few hundred meters to one kilometer. Designation of each snow site as local or regional was based on an analysis of topography and land-cover maps and the observer's notes about snowpack variability, surrounding topography and vegetation. For the year with the most extensive snow survey measurements (2009), 54 sites fall within the local category and 89 sites were classified as representing regional snow variability.

As mentioned above, not all of these sites were visited prior to or after 2009 (Figure 4; Table 2), and this resulted in a selection of so-called 'long-term' regional sites. These sites are highlighted in grey on Figure 1. The total number of long-term regional sites visited each year from 1996 to 2011 is summarized in Table 2.

Variability in the snow water equivalent

Long-term regional sites were examined to determine the temporal trends in SWE data. The period of analysis was limited to 2000–2011 since, in the earlier years of 1996–1999, there were very few sites (one to four sites, Table 2). The averaged SWE for the entire domain ranges from 92 mm in 2008 to 148 mm in 2011. This number represents the total precipitation (less sublimation) from October to April. Figure 5(a) shows that the SWE variation from year to year is much less than SWE variation within the domain during 1 year. The standard deviation of SWE within the domain is 26–47 mm, whereas the standard deviation for averaged SWE from year to year is only 16 mm. The largest range of SWE variation from year to year is observed during recent years.

Observations indicate that 2009 and 2011 are the years with highest SWE of 141 and 148 mm, respectively. The end-of-winter SWE for 2009 and 2011 accounts for 124 and 131% of the 12-year mean SWE (113 mm). The 2008 end-of-winter SWE represents 81% of the 12-year mean SWE; 2006 accounts for 88% of the 12-year mean SWE (Table 2). It is notable that recent years exhibit both extreme high (2009 and 2011) and extreme low (2008) snow accumulation. These recent years with high SWE can cause a positive trend in the data; however, the large standard deviations and short period of record make a trend analysis ill advised.

The observation of extreme SWEs during recent years raises the question of whether a similar pattern of high and low snow accumulation can be seen in nearby regions

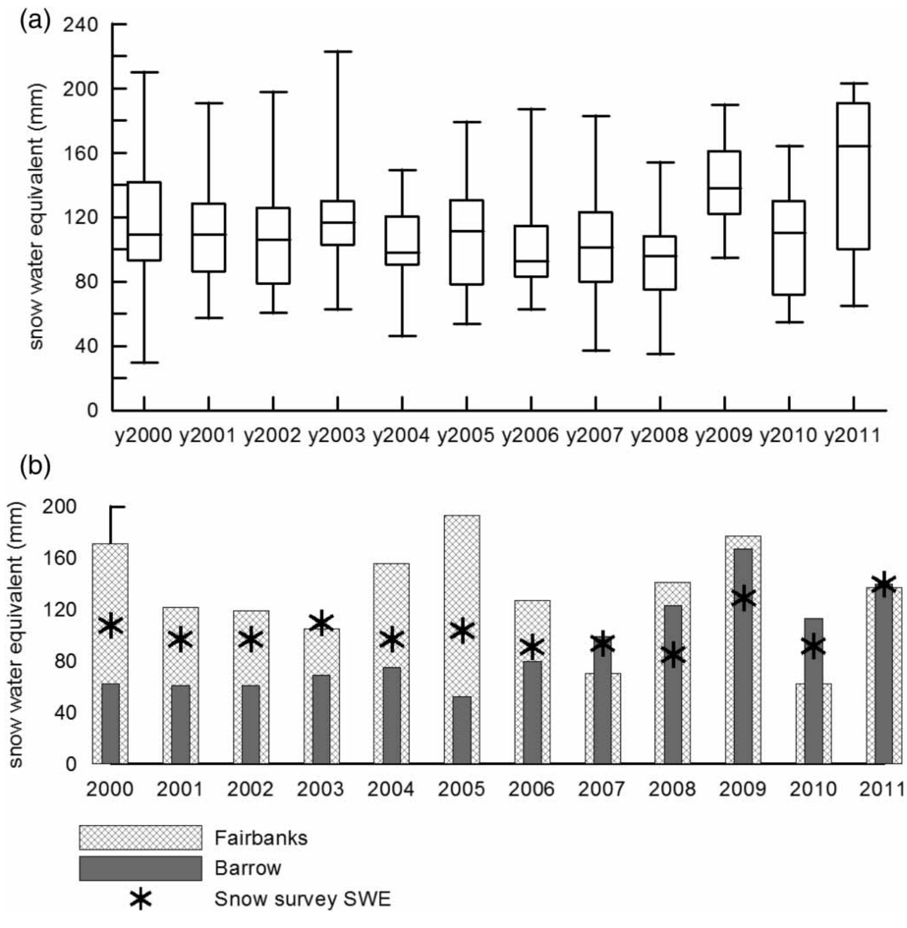

Figure 5 | (a) Box and whisker plot showing median, minimum, maximum, lower quartile, and upper quartile for the SWE from 2000 to 2011. (b) Snowfall accumulated from October to April at primary NWS stations in Fairbanks and Barrow. Stars show SWE averaged from long-term regional snow surveys.

of Alaska. In the case of this research domain, the closest climate records from National Weather Service (NWS) primary stations are Barrow (Arctic) and Fairbanks (Interior Alaska). We summed snowfall records for each winter from October to April and converted the numbers to the SWE by assuming the density of freshly fallen snow is 100 kg m^{-3}. Similar tendencies of high SWE in recent years were found in Barrow, but were not seen at Fairbanks in Interior Alaska (Figure 5(b)). If we extend the record to 1960, there appears to be no climatic similarity between the Fairbanks and Barrow snowfall datasets (Figure 6). We can see on Figure 6 that winter of 2009 had the highest accumulated snowfall at Barrow. Barrow records start in 1908, but there is a large percentage of missing records before 1960.

Assimilation of snow water equivalent data

The usefulness of the observed snow data for improving our representation of spatial snow distributions can be demonstrated with the SnowModel (Liston & Elder 2006) and SnowAssim (Liston & Hiemstra 2008) snow data assimilation scheme. The physically based, spatially distributed SnowModel has been widely applied across the different landscapes of the world to simulate snow-related processes. Model development and applications are well documented in many publications (Liston & Elder 2006; Liston et al. 2007; Liston & Hiemstra 2008). Physically based models

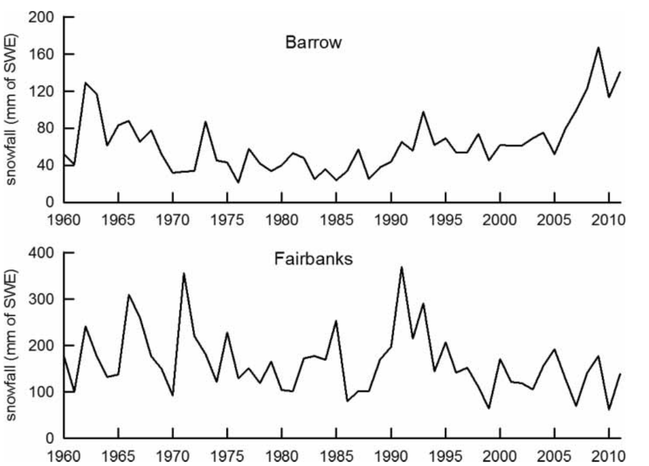

Figure 6 | Snowfall accumulated from October to April each year in Barrow and Fairbanks. Snowfall was converted to SWE by assuming a density of freshly fallen snow of 100 kg m^{-3}. Note that the scale of vertical axis for Barrow differs from that for Fairbanks by a factor of 2.

generally perform the best in data-rich regions, where measurements of precipitation (P), air temperature (T), relative humidity (RH), wind speed (WS) and direction (WD) provide reliable forcing across the landscape. This data-gathering is not often possible in the remote Arctic environment, where information on solid precipitation is inadequate due to the nature of the gauge design and its interaction with the wind and snow (Goodison et al. 1998; Yang et al. 2000). Under these conditions, snow on the ground becomes viable input that allows the model to constrain errors associated with the precipitation data (Liston & Sturm 2002).

SnowModel simulations were performed for a 280 × 286 km domain (see Figure 1) for the winter season of 1 September 2008–15 June 2009. Input data included US Geological Survey (USGS) smoothed digital elevation data, national land cover data, snow survey data and T, WS, WD and RH from the meteorological stations shown in Figure 1. Observed winter precipitation was taken from three USDA Natural Resources Conservation Service (NRCS) SNOTEL (snowpack telemetry) sites distributed across the domain from south to north: Imnavait, Sagwon and Prudhoe Bay. Spatial SWE distributions were produced every day for the 2,800 × 2,860 grid cells. Each grid cell is 100 m × 100 m.

First, a spatial SWE distribution was produced by interpolating SWE observations with the inverse-distance-weighted technique in ArcMap (Figure 7(a)). Model simulations for the Alaska Arctic were then performed similarly to the description in Liston & Hiemstra (2008) for two configurations: (1) model-simulated snowpack evolution without data assimilation scheme; and (2) model-simulated snowpack evolution with the data assimilation scheme that utilizes observed SWE. Results of the SnowModel simulations with the data assimilation are shown in Figure 7(b) as spatially distributed SWE on 21 April 2009. SWE observations, assimilated in SnowModel, were plotted over the modeled SWE using an identical color scheme, where the observational dots are surrounded by a black circle (Figure 7(b)). It can be seen that SWE observations combined with the SnowModel provide much more detail on the spatial snow distribution when compared with the interpolated SWE. As an example, spatial heterogeneity in the SWE distribution is clearly

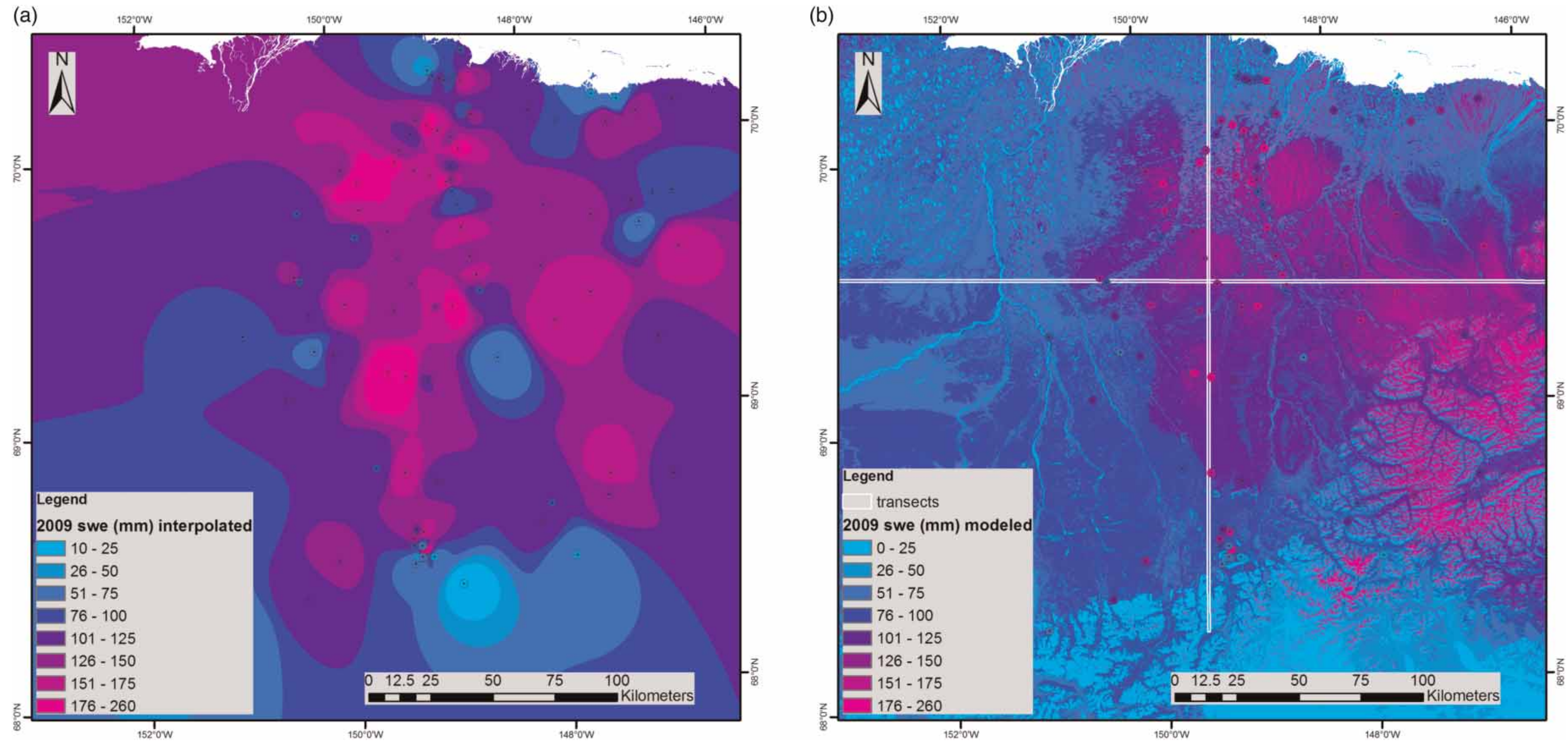

Figure 7 | (a) Interpolated and observed (dots) and (b) modeled and observed (dots) SWE on 21 April 2009. Size of the domain is identical to Figure 1.

seen on the coastal plain, where river ice and lake ice show lower SWE when compared with the tundra SWE nearby. Lakes are visible in light-blue color along the coast.

Both model results and observations highlight areas of high SWE on the leeward slopes of White Hills and Franklin Bluffs and the decrease in SWE near the coast. The Brooks Range has areas of high SWE at the east end and areas of low SWE at the south of the simulation domain. These spatial trends are also seen on the SWE bands extracted from the modeled SWE distributions (Figures 8(a) and (b)). The location of these bands is shown in Figure 7(b), where each band is 1 km wide and includes 10 grid cells. Averaged SWE across the band is plotted from the coast to the Brooks Range (Figure 8(a)) and from west to east (Figure 8(b)). SWE extraction was performed from the two modeled results with the assimilation of snow survey data and without assimilation of snow survey data. The SWE generally increases from west to east around the White Hills and the foothills of the Brooks Range (Figures 7(b) and 8(b)). Both model results and observations generally indicate lower SWE in the south part of the domain, increasing SWE in the central part and a decrease in SWE close to the coast (Figures 7(b) and 8(a)).

Modeled SWE with the assimilated snow data is significantly higher when compared with SWE distributions produced without data assimilation (Figure 8(b)). A comparison of Figure 7(a) and Figure 7(b) clearly shows that snow observational data, when assimilated in the physically

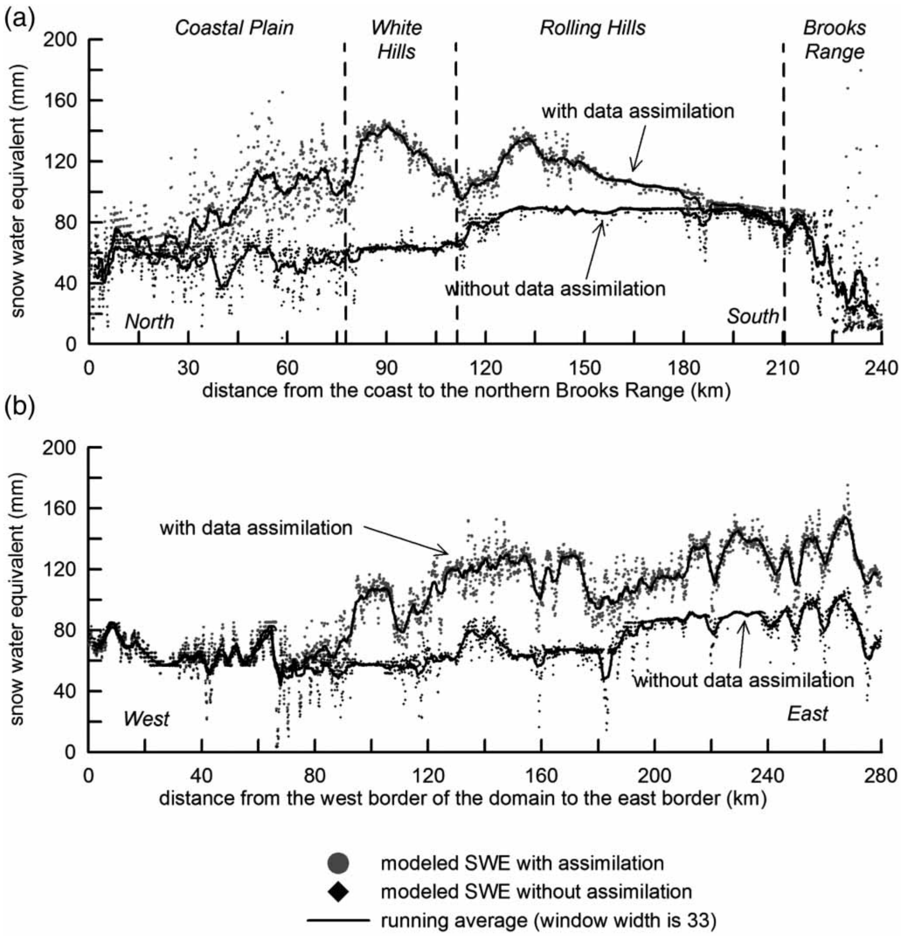

Figure 8 | Comparison of model SWE with and without assimilation of observational data. Modeled SWE was extracted for 21 April 2009, along the (a) north-south and (b) west-east bands. Location of these bands is shown in Figure 7(b). Each band is 1 km wide and includes 10 grid cells. Grey dots indicate averaged SWE across the band; corresponding lines show running average.

based models, significantly improves the performance of SnowModel in the areas with poor winter precipitation data.

DISCUSSION

Worldwide, many surface-based snow-observation networks have diminished or have been completely lost; those that remain provide valuable snow observations (IGOS 2007). Previous systematic snow measurements of large regional extent had not been performed repeatedly in the Alaska Arctic for more than a few years. In the past, intensive sampling traverses from the Brooks Range to the Beaufort Sea coast provided rich information on spatial distribution of snow depth, SWE and snowpack stratigraphy (Liston & Sturm 2002; Sturm *et al.* 2010), yet these traverses had an episodic character and often explored different areas of the north. The most systematic SWE data collection has been maintained by the US Department of Agriculture (USDA) since the 1970s; however, this collection is based only on a few point measurements collected along the Dalton Highway (McClure *et al.* 2009).

Such snow observations, and those presented here, are key components of many scientific and engineering applications. For example, local snow sites can provide useful input for spatially distributed hydrologic models of small watersheds (Ferguson 1999; Zhang *et al.* 2000; Clark *et al.* 2011). As mentioned above, the presence of deep snowdrifts extends the duration of snowmelt (Hinzman *et al.* 1990), whereas the SWE-related mosaic of bare and snow-covered ground has important climate and hydrologic system implications during the snowmelt period. Understanding and modeling these processes require spatially distributed SWE data and knowledge of micro- to macro-scale snow variability.

Large spatial coverage of snow survey sites may provide sufficient information for validation of SWE estimates from airborne and satellite-based remote sensors (Koenig & Forster 2004; Derksen *et al.* 2010; Voglmeir 2011). As an example, snow survey sites in the Kuparuk River basin were used to evaluate Special Sensor Microwave Imager (SSM/I) SWE retrieval algorithms for the shallow snowpack (Koenig & Forster 2004). An important consideration for these types of applications is how to bridge the gap in spatial scales between ground observations and remote sensing imagery. The combination of a physically based model, with the assimilation of snow observations, can provide a useful tool to address spatial scale questions (Liston & Hiemstra 2008).

CONCLUSIONS

Among the long-recognized challenges of pan-Arctic snow studies, the two issues that stand out are the spatially sparse observational network and variations in that network over time. In this paper, we address these two issues by introducing a long-term observational snow dataset in the Alaska Arctic that relies on *in situ* data consistent in time (repeated measurements every year) and in space (sites are distributed over a large area).

The data collection was initiated in 1985 in the small Imnavait Creek watershed just north of the Brooks Range. Over the years, data collection extended to include the Upper Kuparuk River watershed in the early 1990s, the entire Kuparuk River watershed in the late 1990s and then the adjacent watersheds in 2000s. As of today, the entire collection includes meteorological, soil, snow and streamflow data that are available to study physical processes unique to Arctic hydrology (Hinzman *et al.* 1990; Lilly *et al.* 1998; Kane *et al.* 2000; Kane & Yang 2004; Hinzman *et al.* 2005).

The averaged SWE for the entire domain ranged from 92 mm in 2008 to 148 mm in 2011 during the last 12 years of records. Temporal variations in averaged SWE from year to year are much less than spatial variations in SWE within 1 year. The standard deviation of SWE within the domain was 26–47 mm, whereas the standard deviation for averaged SWE from year to year was only 16 mm. It is notable that recent years exhibit both the extreme high (2009 and 2011) and the extreme low (2008) snow accumulation. Similar tendencies of high SWE in recent years were found in Barrow, but were not seen in Interior Alaska (Fairbanks). Climatic records of snowfall from Barrow also indicate that 2009 had the highest snowfall accumulation during 1960–2011.

Spatial snow variability was studied for 1 year (2009) with high-resolution snow distributions produced by merging observed SWE with the SnowModel/SnowAssim snow evolution modeling system, thus providing valuable information on snow variability at meso- and macro-scales. The spatial pattern shows lower SWE in the west and south, increasing SWE from west to east in the Foothills and a decrease in SWE from Foothills toward the coast. The spatial pattern looks different when observational SWE is not assimilated in the SnowModel. This difference emphasizes that snow observational data significantly improve model performance in Arctic areas with limited and/or poor winter precipitation data.

ACKNOWLEDGEMENTS

The faculty, staff and students of Water and Environmental Research Center, University of Alaska Fairbanks collect snow data each year; their work and dedicated contribution over the years is greatly acknowledged. Special thanks are directed to Dr Chris Hiemstra for the assistance with land cover data preparation and Dr Daqing Yang for insightful comments. This work was supported through National Science Foundation, Office of Polar Programs, Arctic Observing Network grants 0335941 and 0632160. During recent years, data collection in the eastern and western areas was made possible by grants from Alaska Department of Transportation and Public Facilities and Alaska Department of Natural Resources.

REFERENCES

ACIA 2005 *Arctic Climate Impact Assessment–Scientific Report*. Cambridge University Press, Cambridge.

Benson, C. S. 1982 Reassessment of Winter Precipitation on Alaska's Arctic Slope and Measurements on the Flux of Wind-Blown Snow. Report of the Geophysical Institute. University of Alaska Fairbanks.

Benson, C. S. & Sturm, M. 1993 Structure and wind transport of seasonal snow on the Arctic Slope of Alaska. *Annals of Glaciology* **18**, 261–267.

Berezovskaya, S. & Kane, D. L. 2007 Strategies for measuring snow water equivalent for hydrological applications: Part 1, accuracy of measurements. *Proceedings of 16th Northern Research Basin Symposium*, Petrozavodsk, Russia, 22–35.

Brown, R. D. & Robinson, D. A. 2011 Northern Hemisphere spring snow cover variability and change over 1922–2010 including an assessment of uncertainty. *The Cryosphere* **5**, 219–229.

Chapin, F. S., Sturm, M., Serreze, M. C., McFadden, J. P., Key, J. R., Lloyd, A. H., McGuire, A. D., Rupp, T. S., Lynch, A. H., Schimel, J. P., Beringer, J., Chapman, W. L., Epstein, H. E., Euskirchen, E. S., Hinzman, L. D., Jia, G., Ping, C. L., Tape, K. D., Thompson, C. D. C., Walker, D. A. & Welker, J. M. 2005 Role of land-surface changes in Arctic summer warming. *Science* **310**, 657–660.

Christensen, J. H., Hewitson, B., Busuioc, A., Chen, A., Gao, X., Held, I., Jones, R., Kwon, W.-T., Laprise, R., Magnana-Rueda, V., Mearns, L., Menedez, C. G., Raisanen, J., Rinke, A., Kolli, R. K., Sarr, A. & Whetton, P. 2007 Regional climate projections. In *Climate Change 2007: The Physical Science Basis* (S. Solomon, D. Qin, M. Manning, Z. Chen, M. Marquis, K. B. Averyt, M. Tignor & H. L. Miller, eds). Cambridge University Press, Cambridge, UK and New York, USA, pp. 847–940.

Clark, M. P., Hendrikx, J., Slater, A. G., Kavetski, D., Anderson, B., Cullen, N. J., Kerr, T., Örn Hreinsson, E. & Woods, R. A. 2011 Representing spatial variability of snow water equivalent in hydrologic & land-surface models: a review. *Water Resources Research* **47**, 1–23.

Derksen, C., Toose, P., Rees, A., Wang, L., English, M., Walker, A. & Sturm, M. 2010 Development of a tundra-specific snow water equivalent retrieval algorithm for satellite passive microwave data. *Remote Sensing of Environment* **114** (8), 1699–1709.

Deser, C., Thomas, R., Alexander, M. & Lawrence, D. 2009 The seasonal atmospheric response to projected arctic sea ice loss in the late 21st century. *Journal of Climate* **23**, 333–351.

Euskirchen, E. S., McGuire, A. D. & Chapin, F. S. 2007 Energy feedbacks of northern high-latitude ecosystems to the climate system due to reduced snow cover during 20th century warming. *Global Change Biology* **13**, 2425–2438.

Ferguson, R. I. 1999 Snowmelt runoff models. *Progress in Physical Geography* **23**, 205–227.

Goodison, B. E., Louie, P. Y. T. & Yang, D. 1998 *WMO Solid Precipitation Measurement Inter-Comparison*. WMO Report No. 67.

Hinzman, L. D., Bettez, N. D., Bolton, W. R., Chapin, F. S., Dyurgerov, M. B., Fastie, C. L., Griffith, B., Hollister, R. D., Hope, A., Huntington, H. P., Jensen, A. M., Jorgenson, T., Kane, D. L., Klein, D. R., Kofinas, G., Lynch, A. H., Lloyd, A. H., McGuire, A. D., Nelson, F. E., Oechel, W. C., Osterkamp, T. E., Racine, C. H., Romanovsky, V. E., Stone, R. S., Stow, D. A., Sturm, M., Tweedie, C. E., Vourlitis, G. L., Walker, M. D., Walker, D. A., Webber, P. J., Welker, J. M., Winker, K. S. & Yoshikawa, K. 2005 Evidence and implications of recent climate change in northern Alaska and other arctic regions. *Climatic Change* **72**, 251–298.

Hinzman, L. D., Kane, D. L. & Gieck, R. E. 1990 Regional snow ablation in the Alaskan Arctic. In: *Northern Hydrology: Selected Perspectives* (T. D. Prowse & C. S. L. Ommanney, eds), Proceedings of Northern Hydrology Symposium, Saskatoon, Saskatchewan, pp. 121–139.

IGOS 2007 *Integrated Global Observing Strategy Cryosphere Theme Report: For the Monitoring of our Environment from*

Space & from Earth. Geneva, World Meteorological Organization. WMO/TD-No.1405.

IPCC 2007 Climate change 2007 The physical science basis. In: *Contribution of Working Group I to the Fourth Assessment Report of the Intergovernmental Panel on Climate Change* (S. Solomon, D. Qin, M. Manning, Z. Chen, M. Marquis, K. B. Averyt, M. Tignor & H. L. Miller, eds). Cambridge University Press, Cambridge, UK and New York, USA.

Kane, D. L., Hinzman, L. D., Benson, C. S. & Liston, G. E. 1991 Snow hydrology of a headwater arctic basin 1. Physical measurements & process studies. *Water Resources Research* **27**, 1099–1109.

Kane, D. L., Hinzman, L. D., McNamara, J. P., Zhang, Z. & Benson, C. S. 2000 An overview of nested watershed study in Arctic Alaska. *Nordic Hydrology* **31**, 245–266.

Kane, D. L., Luthin, J. N. & Taylor, G. S. 1978 *Heat and Mass Transfer in Cold Regions Soils*. IWR-65, Institute of Water Resources, University of Alaska Fairbanks.

Kane, D. L. & Yang, D. 2004 *Northern Research Basins Water Balance*. IAHS Publication 290, Wallingford, UK.

Koenig, L. & Forster, R. 2004 Evaluation of passive microwave snow water equivalent algorithms in the depth hoar-dominated snowpack of the Kuparuk River watershed, Alaska, USA. *Remote Sensing of Environment* **93**, 511–527.

Lilly, E. K., Kane, D. L., Hinzman, L. D. & Gieck, R. E. 1998 Annual water balance for three nested watersheds on the north slope of Alaska. In: *Proceedings, Seventh International Conference on Permafrost* (A. G. Lewkowicz & M. Allard, eds), Yellowknife, Canada, pp. 669–674.

Liston, G. E. 1995 Local advection of momentum, heat, & moisture during the melt of patchy snow covers. *Journal of Applied Meteorology* **34**, 1705–1715.

Liston, G. E. 1999 Interrelationships among snow distribution, snowmelt, and snow cover depletion: implications for atmospheric, hydrologic, and ecologic modeling. *Journal of Applied Meteorology* **38**, 1474–1487.

Liston, G. E. 2004 Representing subgrid snow cover heterogeneities in regional and global models. *Journal of Climate* **17**, 1381–1397.

Liston, G. E. & Sturm, M. 2002 Winter precipitation pattern in Arctic Alaska determined from a blowing-snow model & snow-depth observations. *Journal of Hydrometeorology* **3**, 646–659.

Liston, G. E. & Elder, K. 2006 A distributed snow-evolution modeling system (SnowModel). *Journal of Hydrometeorology* **7**, 1259–1276.

Liston, G. E. & Hiemstra, C. A. 2008 A simple data assimilation system for complex snow distributions (SnowAssim). *Journal of Hydrometeorology* **9**, 989–1004.

Liston, G. E. & Hiemstra, C. A. 2011 The changing cryosphere: Pan-Arctic snow trends (1979–2009). *Journal of Climate* **24**, 5691–5712.

Liston, G. E., Haehnel, R. B., Sturm, M., Hiemstra, C. A., Berezovskaya, S. & Tabler, R. D. 2007 Simulating complex snow distributions in windy environments using SnowTran-3D. *Journal of Glaciology* **53**, 241–256.

Marsh, P. & Pomeroy, J.W. 1995 Water & energy fluxes during the snowmelt period at an Arctic treeline site. *International GEWEX workshop on Cold Season/Region Hydrometeorology. International GEWEX project office publ. series* **15**, 197–201.

McClure, R., Montesi, J. & Kenney, D. 2009 *Alaska Snow Survey Report*, USDA Natural Resources Conservation Service, Anchorage, Alaska.

McGuire, A. D., Anderson, L. G., Christensen, T. R., Dallimore, S., Guo, L. D., Hayes, D. J., Heimann, M., Lorenson, T. D., Macdonald, R. W. & Roulet, N. 2009 Sensitivity of the carbon cycle in the Arctic to climate change. *Ecological Monographs* **79**, 523–555.

McKay, G. A. & Gray, D. M. 1981 Distribution of snow cover. In *Chapter 5 in Handbook of Snow* (D. M. Gray & D. H. Male, eds), Pergamon Press, IAHS Press, Wallingford, UK, pp. 153–190.

Olsson, P. Q., Hinzman, L. D., Sturm, M., Liston, G. & Kane, D. L. 2002 *Surface Climate & Snow-Weather Relationships of the Kuparuk Basin on Alaska's Arctic Slope*. ERDC/CRREL Technical Report TR-02–10. US Army Corps of Engineers.

Räisänen, J. 2008 Warmer climate: less or more snow? *Climate Dynamics* **30**, 307–319.

Romanovsky, V. E., Sazonova, T. S., Balobaev, V. T., Shender, N. I. & Sergueev, D. O. 2007 Past and recent changes in permafrost and air temperatures in Eastern Siberia. *Global & Planetary Change* **56**, 399–413.

Rovansek, R. J., Kane, D. L. & Hinzman, L. D. 1993 Improving estimates of snowpack water equivalent using double sampling. *Proceedings of the 61st Western Snow Conference*, pp. 157–163.

Serreze, M. C., Walsh, J. E., Chapin, E. C., Osterkamp, T., Dyugerov, M., Romanovsky, V., Oechel, W. C., Morison, J., Zhang, T. & Barry, R. G. 2000 Observation evidence of recent change in the northern high-latitude environment. *Climate Change* **46**, 159–207.

Shiklomanov, A. I., Lammers, R. B. & Vörösmarty, C. J. 2002 Widespread decline in hydrological monitoring threatens Pan-Arctic research. *EOS, Transactions of the American Geophysical Union* **83**, 13.

Shook, K., Gray, D. M. & Pomeroy, J. W. 1993 Temporal variation in snow cover area during snowmelt in prairie & alpine environments. *Nordic Hydrology* **24**, 183–198.

Skoien, J. O. & Bloschl, G. 2006 Sampling scale effects in random fields and implications for environmental monitoring. *Environmental Monitoring and Assessment* **114**, 521–552.

Slaughter, C. W. & Benson, C. S. 1986 Seasonal snow and aufeis in Alaska's taiga. *Proceedings: Cold Regions Hydrology American Water Resources Association*, Bethesda, MD, pp. 101–109.

Slaughter, C. W. & Kane, D. L. 1979 Hydrologic role of shallow organic soils in cold climates. *Proceedings of the Canadian Hydrology Symposium: Cold Climate Hydrology*, Vancouver, BC. National Research Council of Canada, Ottawa, pp. 380–389.

Stroeve, J., Serreze, M., Drobot, S., Gearheard, S., Holland, M., Maslanik, J., Meier, W. & Scambos, T. 2008 Arctic sea ice extent plummets in 2007. *Eos Transactions of AGU* **89**, 13–20.

Sturm, M. & Benson, C.S. 2004 Scales of spatial heterogeneity for perennial and seasonal snow layers. *Annals of Glaciology* **38**, 253–260.

Sturm, M., Taras, B., Liston, G. E., Derksen, C., Jonas, T. & Lea, J. 2010 Estimating snow water equivalent using snow depth data and climate classes. *Journal of Hydrometeorology* **11**, 1380–1394.

Voglmeir, K. 2011 Retrieval of Snow Characteristics by QuikSCAT Backscatter Measurements over North Slope, Alaska. MSc Thesis, University of Innsbruck, Austria.

White, D., Hinzman, L., Alessa, L., Cassano, J., Chambers, M., Falkner, K., Francis, J., Gutowski, W. J., Holland, M., Holmes, R. M., Huntington, H., Kane, D., Kliskey, A., Lee, C., McClelland, J., Peterson, B., Rupp, T. S., Straneo, F., Steele, M., Woodgate, R., Yang, D., Yoshikawa, K. & Zhang, T. 2007 The arctic freshwater system: Changes and impacts. *Journal of Geophysical Research-Biogeosciences* **112**, G04S54.

Woo, M-K. 1997 *A Guide for Ground Based Measurement of the Arctic Snow Cover*. Canadian Snow Data CD, Meteorological Service of Canada, Downsview, Ontario, pp. 30.

Work, R. A., Stockwell, H. J., Freeman, T. G. & Beaumont, R. T. 1965 *Accuracy of Field Snow Surveys in Western United States Including Alaska*. Technical report 163, US Army CRREL, Hannover, NH, 43 p.

Yang, D., Kane, D. L., Hinzman, L. D., Goodison, B. E., Metcalfe, J. R., Louie, P. Y., Leavesley, G. H., Emerson, D. G. & Hanson, C. L. 2000 An evaluation of the Wyoming gauge system for snowfall measurement. *Water Resources Research* **36** (9), 2665–2677.

Zhang, Z., Kane, D. L. & Hinzman, L. D. 2000 Development and application of a spatially distributed Arctic Hydrological & Thermal Process Model (ARHYTHM). *Hydrological Processes* **14**, 1017–1044.

First received 15 November 2011; accepted in revised form 22 May 2012. Available online 28 July 2012